

Estimation of Intra-vitreous Half-Lives in the Rabbit Eye with Semi-mechanistic Equations

Walter Schmitt¹ 

Received: 14 June 2016 / Accepted: 2 September 2016 / Published online: 14 September 2016
© Springer Science+Business Media New York 2016

ABSTRACT

Purpose To develop an alternative method for estimating vitreous half-lives in the rabbit eye based on simple equations for the physical processes of dissipation and the physicochemical properties of therapeutic substances applied by intravitreal drug administration.

Methods Equations were derived to describe diffusion in the vitreous humor and permeation through the back-of-the-eye tissue, and the volume of distribution. The model was validated using reported half-life values from 83 compounds collected from literature.

Results The rate limiting step for dissipation from the vitreous depends mainly on the molecular weight. Dissipation of very low molecular weight (MW) substances (<350 Da) is limited by diffusional transport to the back of the eye, for substances with a MW >350 Da uptake into the back of the eye tissue becomes limiting, and large molecules >500 Da predominantly take an alternative path being cleared through the front of the eye for which diffusion towards the posterior chamber turns out to be limiting. Taking the three rate determining processes into account, the derived model can estimate dissipation rates and respectively vitreous half-life values of small compounds and macromolecules from their molecular weight with very few exceptions.

Conclusions The equations derived in this analysis provide a simple method to predict vitreous half-lives for a diverse group of molecules and can be easily implemented in early drug development.

KEY WORDS half-life · intravitreal · ocular · ocular pharmacokinetics · rabbit eye

ABBREVIATIONS

A	Cross section area
BoE	Back of eye
CFD	Computational fluid dynamics
D	Diffusion coefficient
d	Distance of diffusion path
Da	Dalton
eta	Viscosity of the liquid
f	Fraction
fu	Fraction unbound
IVT	Intravitreal
k _B	Boltzmann constant
k _{diss}	Dissipation rate
K _{m:w}	Membrane/water partition coefficient
K _{o:w}	Octanol/water partition coefficient
K _{p:w}	Protein/water partition coefficient
K _{v:w}	Vitreous/water partition coefficient
MW	Molecular weight
P	Permeability
PC	Physicochemical
QSPKR	Quantitative Structure-Pharmacokinetic Relationships
r	Radius
R ₀	Hydrodynamic radius of the diffusing particle
T	Temperature

Electronic supplementary material The online version of this article (doi:10.1007/s11095-016-2037-7) contains supplementary material, which is available to authorized users.

✉ Walter Schmitt
walter.schmitt@bayer.com

¹ Clinical Science, Bayer Pharma AG, Wuppertal, Germany

$t_{1/2}$	Half-life
V_d	Volume of distribution
V_{vit}	Volume of the vitreous

INTRODUCTION

Age-related macular degeneration, diabetic retinopathies, glaucoma, and rare retinal degenerations are vision impairing disorders that affect the posterior region of the eye (1). Ensuring that therapeutic substances come into contact with the affected region for an adequate amount of time is a significant challenge when treating these conditions. Currently, intravitreal (IVT) drug administration is the state of the art option for administering drugs to the vitreous. This allows therapeutic concentrations of the substances to reach the vitreous humor, retina and choroid regions of the eye and it has been shown to be superior over systemic approaches (2). However, due to the invasive nature of this method, it is desirable to have compounds with long residence times or to use depot formulations with controlled release so that the therapeutic substance remains in contact with the affected area of the eye for an adequate amount of time and to minimize the number of drug administrations that are required. Therefore, the vitreal half-life of a therapeutic agent is an important factor for the optimization of drug substances and formulations.

The vitreal half-life is dependent upon the physicochemical properties of intraocular substances, such as molecular weight, lipophilicity, and solubility, as well as the processes of dissipation once the substance is injected. After a drug is administered to the vitreous humor, elimination is carried out either anteriorly by simple diffusion to the posterior chamber, followed by removal to the system circulation along with the aqueous humor drainage, or posteriorly across the retina where it is removed by active secretion (3).

Determining the intravitreal half-life of drugs *in vivo* is time and animal consuming, as well as cost intensive. Therefore, a number of methods have been proposed to estimate vitreal half-lives using quantitative approaches. These include visual correlation (4), Quantitative Structure-Pharmacokinetic Relationships (QSPKR) with multi-linear regression (5,6), and computational fluid dynamics (CFD) (7–10). These approaches, however, either only take the drug properties into consideration without including the mechanistic component of dissipation within the eye or involve very complicated quantitative models. QSPKR assumes the same linear dependence over the entire parameter range, which may not be realistic or valid. CFD methods are only useful for experts and are therefore usually not applicable during drug development. Moreover, this approach does not normally allow direct conclusions to be made about the relation between substance properties and behavior. This can only be investigated with dedicated simulations where the input parameters are

systematically varied. Therefore, a method is desirable that is easy to use, mathematically describes the transport processes in the eye and provides a direct insight into the relation between compound properties and vitreal half-lives.

An understanding of the relationship between the physicochemical properties of the therapeutic agents and the drug elimination process from the vitreous is essential for predicting vitreal half-lives. A simplified and accurate method of estimating half-lives before animal studies are carried out would be useful for designing new drug molecules for treating ocular diseases and would reduce the number of animals needed for pre-clinical studies. The objective of this manuscript is to provide a mechanistic understanding of the dissipation of substances from the vitreous and its correlation to physicochemical properties of the substances. It describes an alternative method for estimating vitreal half-lives in the rabbit eye based on simple equations describing the physical processes of dissipation by considering the physicochemical properties of therapeutic substances. The resulting model is tested and calibrated using data on 83 substances collected from literature sources.

MATERIALS AND METHODS

Data Collection for Intravitreal Half-Lives and Physicochemical Properties

Half-life values after IVT application were collected from published literature for 83 compounds (4–6,11–14). All of the studies were conducted exclusively in rabbits and data from both the albino strain and the pigmented rabbit strain were included. The data set is comprised of small molecules as well as macromolecules.

Terminal half-life, respectively dissipation rate values were taken directly from the publications. Several of the sources used are articles also reviewing and evaluating results from previous research. In some of these cases the list of drugs and the references overlap. In these cases only one of the reported half-life values was used and preference was given to the reference reporting the original value without re-evaluation. If not directly reported, dissipation rates were calculated from half-life values using the formula $k_{diss} = \ln(2)/t_{1/2}$. In cases where physicochemical (PC) data (i.e. molecular weight and logP) for the substances were reported, these parameters were also derived. If the PC-properties were not available, the values were obtained from the online database DrugBank (15). In case of the logP experimental values were considered if available. Otherwise calculated values were taken from DrugBank.

Derivation of Model Equations for Dissipation Processes

Three processes can principally be considered responsible for the dissipation of drugs from the vitreous. These are a) uptake into the retina-choroid-sclera tissue (in the following named as back of the eye (BoE) tissue) and subsequent absorption into the blood stream or b) transport into the posterior chamber and subsequent evacuation with the aqueous humor and c) degradation within the vitreous. The latter is considered less relevant because the metabolic activity in the vitreous is generally assumed to be low and therefore this process was not considered in the present analysis. For the other two processes it was assumed that the transport within the vitreous humor is solely facilitated by diffusion, disregarding a potential contribution by convection or pressure driven fluid. In case of uptake through the BoE tissue in addition to the diffusion to the border of the vitreous, the uptake into the tissue must be taken into account as the potentially rate limiting process. We considered this to happen by permeation through cell membranes assuming that mainly a transcellular route is taken. For each of the relevant diffusion and permeation processes, indicated in the simplified sketch of a rabbit eye in Fig. 1, the respective transport rates were estimated based on geometric factors and diffusion coefficients in the respective media which depend on substance properties.

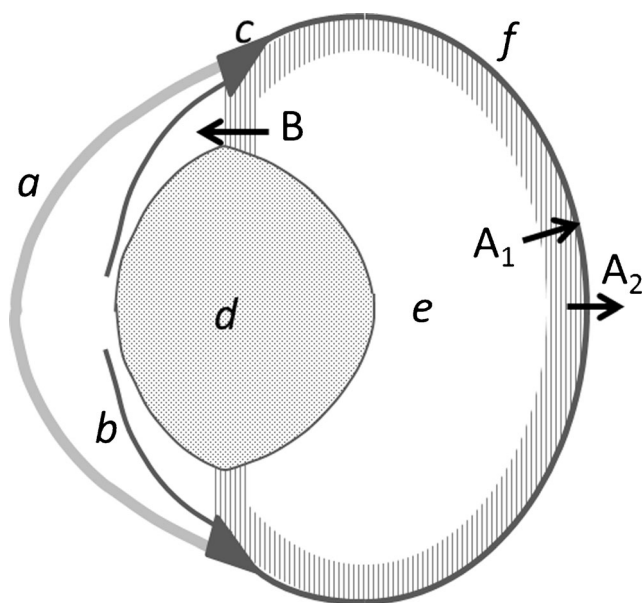


Fig. 1 Schematic cross section of a rabbit eye, indicating the relevant dissipation processes from the vitreous body. A₁: Diffusion to back of the eye. A₂: Uptake and permeation through back of the eye tissue. B: Diffusion to front of the eye and subsequent evacuation with aqueous humor flow. (a): cornea, (b): iris, (c): ciliary body, (d): lens, (e): vitreous body, (f): retina/RPE. The shaded area indicates a layer of the thickness of the mean diffusion length at the surface of vitreous constituting the diffusion barrier for processes A₁ and B.

Diffusion in Vitreous Humor

In order to estimate the rate constant for the radial diffusion in the vitreous to its border (Process A₁ in Fig. 1), the simplifying assumption was made that this process can in first approximation be described by one dimensional diffusion. This is a strongly simplifying assumption considering the complex geometry of the rabbit eye and also neglecting any contribution by convection of pressure driven fluid flows.

According to Fick's law the transport rate for one dimensional diffusion is given by the following formula:

$$k_{diff}^{trans} = \frac{D \cdot A}{d \cdot V_d} \tag{1}$$

With D = diffusion coefficient, A = cross section area, d = length of diffusion path and V_d = volume of distribution.

Also the vitreous humor is considered being a homogenous medium, contrary to other approaches which treat it as a porous medium with diffusion restricted to the pores (10). The diffusion coefficient in homogeneous liquids is given by the Stokes-Einstein-Equation:

$$D = \frac{k_B T}{6\pi\eta R_0} \tag{2}$$

Where k_B = Boltzmann constant, T = absolute temperature, η = viscosity of the liquid and R₀ the hydrodynamic radius of the diffusing particle.

Thus the diffusion coefficient in a viscous medium, e.g. the vitreous, at any temperature can be calculated from the diffusion coefficient in water at 20°C (=293 K) by scaling it according to the respective viscosity and temperature ratios. The coefficient of diffusion in the vitreous humor at body temperature (= 310 K) is therefore calculated as:

$$\begin{aligned} D_{vitreous}(37^\circ C) &= D_{water}(20^\circ C) \frac{\eta_{water}(20^\circ C)}{\eta_{vitreous}(37^\circ C)} \frac{310K}{293K} \text{ cm}^2/\text{s} \\ &= 1.06 D_{water}(20^\circ C) \frac{\eta_{water}(20^\circ C)}{\eta_{vitreous}(37^\circ C)} \text{ cm}^2/\text{s} \end{aligned} \tag{3}$$

The diffusion coefficient of molecules in water at 20°C, on the other hand, can be calculated from their molecular weight. For small molecules the respective equation was derived by calculating the regression line to measured diffusion coefficients (16):

$$D_{water}(20^\circ C) = 10^{-4} MW^{-1/2} \text{ cm}^2/\text{s} \tag{4}$$

For large molecules the respective equation is (16,17):

$$D_{water}(20^\circ C) = 2.74 \cdot 10^{-5} MW^{-1/3} \text{ cm}^2/\text{s} \tag{5}$$

Both equations result in the same value for a molecular weight of 2400 Da. Thus, for the following considerations this molecular weight is considered as the threshold value for switching between Eqs. 4 and 5.

The viscosity of the vitreous humor varies spatially. Abdelkawi determined the viscosity at different locations in the rabbit vitreous (18). In the posterior part, most relevant for the present consideration, the viscosity at 37°C is 1.9 mPa s. Respectively, a scaling factor of 0.53 has to be considered in Eq. 3, leading to:

$$D_{\text{vitreous humor}}(37^\circ\text{C}) = \begin{cases} 5.62 \cdot 10^{-5} MW^{-1/2} \frac{\text{cm}^2}{\text{s}}, & \text{if } MW < 2400 \text{ Da} \\ 1.54 \cdot 10^{-5} MW^{-1/3} \frac{\text{cm}^2}{\text{s}}, & \text{if } MW \geq 2400 \text{ Da} \end{cases} \quad (6)$$

For the estimation of the geometric factors in Eq. 1 again some gross assumption was made. For the mean diffusion path length to the border of the vitreous a spherical geometry was assumed and the mean diffusion length was assumed to be the distance between the radius of the shell including 50% of the volume and the outer shell, resulting in

$$d = \left(1 - \sqrt[3]{0.5} r_{\text{vitreous}}\right) = 0.21 r_{\text{vitreous}} \quad (7)$$

This is based on the additional assumption that the vitreous is well stirred with homogenous distribution of the injected substance. Considering the mean of the long and the short axis of the spheroidal vitreous of the rabbit as its approximated radius ($r = 7.7$ mm, (10)) the estimation of the diffusion length results in $d = 1.7$ mm. The retinal surface area was considered as the surface area A, available for uptake into back of the eye tissue. For rabbits this area was determined to be 6 cm^2 (19). Inserting the values for D, A and d into Eq. 1 results in the following simple equations for calculating the transport rate from the vitreous to the retina:

$$k_{\text{diff BoE}}^{\text{trans}} = \frac{D \cdot A}{d \cdot V_d} = \begin{cases} 1.98 \cdot 10^{-3} \frac{MW^{-1/2}}{V_d} \frac{1}{\text{s}}, & \text{if } MW < 2400 \text{ Da} \\ 5.43 \cdot 10^{-4} \frac{MW^{-1/3}}{V_d} \frac{1}{\text{s}}, & \text{if } MW \geq 2400 \text{ Da} \end{cases} \quad (8)$$

For the anterior pathway (Process B in Fig. 1) the mean diffusion length within the vitreous was assumed to be the same as towards the retina. Therefore only the cross section relevant for the diffusion differs in this case. This area was assumed to be the cross section of the ring shaped aperture between the lens and the ciliary body. Taking into account the radius of the rabbit lens, $r_{\text{lens}} = 4.75$ mm, and the inner

radius of the ciliary body, $r_{\text{ciliary}} = 7$ mm (10), this area accounts to $A = 0.84 \text{ cm}^2$. This then leads to the following transport rates:

$$k_{\text{diff ant}}^{\text{trans}} = \frac{D \cdot A}{d \cdot V_d} = \begin{cases} 2.77 \cdot 10^{-4} \frac{MW^{-1/2}}{V_d} \frac{1}{\text{s}}, & \text{if } MW < 2400 \text{ Da} \\ 7.6 \cdot 10^{-5} \frac{MW^{-1/3}}{V_d} \frac{1}{\text{s}}, & \text{if } MW \geq 2400 \text{ Da} \end{cases} \quad (9)$$

Permeation Through Back of the Eye Tissue

In order to be taken up from the vitreous into systemic blood circulation through the back of the eye tissue, substance injected into the vitreous has to permeate through several cell layers of that tissue (Process A₂ in Fig. 1). The rate determining process in this case is either the permeation through the cell membranes of one of these layers or paracellular diffusion, e.g. through tight junctions in the retinal pigmented epithelium. The latter might be particularly relevant for hydrophilic compounds, as they are primarily represented in the present dataset. More lipophilic substances will rather take the transcellular route. Based on the available data it cannot definitely be determined which of the two types of processes is the dominant one, but the observed vitreal half-lives accounted for a higher probability in favor of the transcellular route. More details are given in the [supplementary material](#). Permeation through cell membranes is, from a physical perspective, also a diffusion process and thus the transport rate for this process is given by an equation similar to the two cases described before. However, since the concentration in the membrane may be different from the concentration in the compartment for which the transport rate is defined, the respective partition coefficient occurs as a factor in the permeability apart from the diffusion coefficient and the thickness of the membrane. Thus the rate of transport through back of the eye is given by:

$$k_{\text{BoE}}^{\text{trans}} = \frac{P \cdot A}{V_d} = \frac{K_{m:w} \cdot D \cdot A}{d \cdot V_d} \quad (10)$$

Where P = permeability, A = surface area, V_d = volume of distribution, D = diffusion coefficient, d = thickness of the membrane and K_{m:w} = membrane:water partition coefficient.

In contrast to the diffusion in the vitreous the surface area available for permeation through the cell membranes, cannot easily be estimated from the eye geometry. It is most likely given by the cellular surface of one of the tissue layers, facing towards the inner of the eye ball and may thus differ strongly from the geometric area of the back of the eye surface. The dependence of cell membrane permeability on molecular weight and lipophilicity of the permeating substances has been

investigated in the past using different experimental approaches (20–22). Thorough, though rather early direct measurements of the uptake of chemicals into different types of cells showed that the diffusion coefficient **D** of cell membranes depends much stronger on molecular weight (MW) than it is the case for diffusion in unstructured fluid (20,22). The relation between **D** and **MW** is given by a power law and the experimentally derived exponents vary between -2.9 and -6 depending on the cell type (22). The only mammalian cells used in the study were erythrocytes where the exponent accounted to -6. Therefore this value was used for the present evaluation and the molecular weight dependent transport rate was calculated as:

$$k_{BoE}^{trans} = \frac{\alpha}{V_d} MW^{-6} \frac{1}{s} \quad (11)$$

The pre-factor α comprises all unknown and not independently derivable factors in Eq. 10. For the present approach it was determined by fitting Eq. 11 to experimental data as described below.

Volume of Distribution

The volume of distribution occurring in Eq. 8, Eq. 9 and Eq. 11 is that of the vitreous body and is given by its physical volume (V_{vit}) multiplied by the ratio of the total concentration in the vitreous and the concentration in the free water. Thus it is determined by the partition coefficient between non-aqueous constituents of the vitreous (i.e. hyaloid acid, collagen and other proteins) and the free water (23). This partition coefficient is the inverse of the unbound fraction ($f_{u,vit}$) of a substance in the vitreous and therefore $V_d = V_{vit}/f_{u,vit}$. The unbound fraction, on the other hand, is correlated with the lipophilicity of a compound unless it specifically binds to a certain protein present in the vitreous.

As described for other tissues (23) the estimate of $f_{u,vit}$ is based on the composition of the vitreous body. At least 95% of the vitreous is made up of water and the remaining fractions are proteins and lipids (24) which determine the partition coefficient of the vitreous matrix. A phospholipid concentration of 181 $\mu\text{g}/\text{mL}$ has been reported for the rabbit vitreous (25). Collagen is the predominant protein in the vitreous and inhomogeneously distributed in the rabbit vitreous. Concentrations in the anterior and the posterior part amount to 955 $\mu\text{g}/\text{mL}$ and 75 $\mu\text{g}/\text{mL}$, respectively (24). Here the value for the posterior part was considered relevant.

The equation for calculating the vitreous/water partition coefficient ($K_{v:w}$) is:

$$K_{v:w} = f_{\text{water}} + f_{\text{lipid}}K_{l:w} + f_{\text{protein}}K_{p:w} \quad (12)$$

Where f_{water} and f_{protein} are the water and protein fractions and $K_{p:w}$ is the protein/water partition coefficient.

The octanol/water partition coefficient $K_{o:w}$ can serve as an approximate substitute for $K_{l:w}$ and also $K_{p:w}$ can be estimated from $K_{o:w}$ (26). However, since $K_{p:w}$ is usually fifty times smaller than $K_{o:w}$, proteins do not considerably contribute to $K_{v:w}$ and Eq. 6 can be simplified to:

$$K_{v:w} = 0.95 + 1.8 \cdot 10^{-4} K_{o:w} \quad (13)$$

And respectively

$$f_{u,vit} = 1/K_{v:w} = (0.95 + 1.8 \cdot 10^{-4} K_{o:w})^{-1} \quad (14)$$

This means that f_u values being considerably lower than 1 can only be expected for compounds with $K_{o:w} > 10^3$ at the pH of the vitreous. However, the compounds in the present dataset are almost all either hydrophilic or of very low lipophilicity at physiological pH. Therefore f_u is generally considered to be 1 and the V_d was set to the physical volume of the rabbit vitreous of 1.4 mL for calculations of dissipation rates.

RESULTS

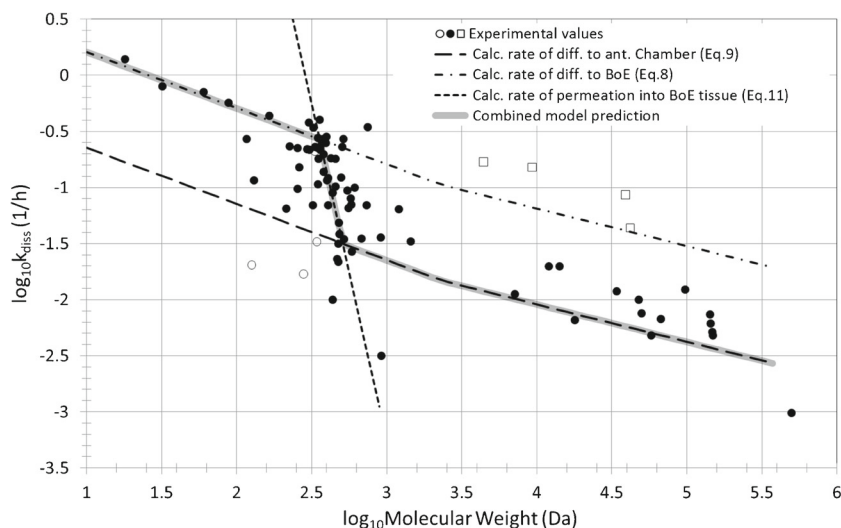
Data Collection for Intravitreal Half-Lives

In total, data for 83 different substances were collected from the literature. For some substances more than one half-life value was found in different publications and in these cases the means of the reported values were used for the present analysis, provided that the values clearly were derived from different experimental studies. The final data set included a wide range of structurally different molecules consisting of 63 small molecules ($MW < 1000$ Da) and 20 macromolecules ($MW > 1000$ Da). The intravitreal half-life values range from 0.5 to 708 h. A table with all data (i.e. half-lives, dissipation rates and characteristics of the substances), as well as the references for each substance, is provided as [supplementary information](#).

Observed Data and Predicted Dissipation Rates

As can be seen from Eq. 8, Eq. 9 and Eq. 11, the dissipation rates for different substances depend mainly on their molecular weight and to a smaller degree on their lipophilicity. Therefore in Fig. 2 the logarithms of the dissipation rates derived from the literature are plotted *vs.* the logarithm of the molecular weight of the substance. The plot clearly shows that the dissipation rates decrease with increasing molecular weight. However, the data points are distributed in a band with a width of about one logarithmic unit, where the rates for small molecules accumulate at the upper boundary of the band while, in contrast, the rates for large molecules are predominantly found at the lower boundary. A transition zone

Fig. 2 Logarithms of rates of dissipation from vitreous body (k_{diss} [1/h]) vs. logarithms of molecular weights. Comparison of observed data (symbols) with values calculated with the calibrated models for diffusion to back of the eye (dash dotted line), permeation through back of the eye tissue (short dashed line) and diffusion towards the posterior chamber (long dashed line). The fat grey line depicts the dissipation rates predicted by the combination of the equations for the three distinct MW ranges. Open circles: substances with very low partition coefficients. Open squares: substances with unexplained high dissipation rates.



between these two subgroups is seen in the range of molecular weights between 250 and 600 Da.

Comparison to the lines which result from the equations for the rate of transport through the vitreous to the retina (Eq. 8) and for the rate of diffusion towards the posterior chamber (Eq. 9), demonstrates that these seem to constitute the upper and lower boundaries of the band in which the data points are lying.

In the narrow range of molecular weights between 350 and 500 Da ($2.54 < \log MW < 2.7$), where about 25% of all data points are located, the rate of dissipation from the vitreous seems to depend much more strongly on molecular weight than on the rates for the diffusion processes as described by the slopes of the lines included in Fig. 2. This may indicate that for the substances in this molecular weight range the permeation through back of the eye tissue is the rate limiting process, for which the exponent of the molecular weight dependence is assumed to be equal to -6 , as discussed above.

Model Calibrations and Final Prediction Model

The factor α in the Eq. 11 was determined by linear regression using the logarithmic values of the observed dissipation rates and logarithmic molecular weights in the MW-range 250 – 600 Da. The resulting fitted line is included in Fig. 2 and shows good agreement with the observed values in the respective molecular weight range. The respective value for α is $2.18 \cdot 10^{11} \text{ cm}^3(\text{g/mol})^6/\text{s}$.

Diffusion to back-of-the-eye and uptake into BoE tissue are serial processes and therefore for the posterior dissipation through BoE the lower of the two respective transport rates is limiting the dissipation of a substance from the vitreous. Whereas the higher of the two transport rates for the parallel

anterior and posterior dissipation routes, estimated for a certain compound, is the overall dominating rate and determines in which direction the substance is cleared. Following this logic the following combined prediction model can be constructed from Eqs. 8, 9 and 11 considering the calibrated value for α in Eq. 11 and assuming $V_d = 1.4 \text{ cm}^3$:

$$k_{\text{diss}} = \begin{cases} 1.41 \cdot 10^{-3} MW^{-\frac{1}{2}} \frac{1}{s}, & MW < 350 \text{ Da} \\ 1.56 \cdot 10^{11} \cdot MW^{-6} \frac{1}{s}, & 350 \leq MW < 500 \text{ Da} \\ 1.97 \cdot 10^{-4} MW^{-\frac{1}{2}} \frac{1}{s}, & 500 \leq MW < 2400 \text{ Da} \\ 5.42 \cdot 10^{-5} MW^{-\frac{1}{3}} \frac{1}{s}, & MW \geq 2400 \text{ Da} \end{cases} \quad (15)$$

k_{diss} values calculated with Eq. 15 are also shown in Fig. 2. In case V_d is known to be considerably different from the geometric volume of the vitreous for a certain substance, it can be considered in the prediction by multiplying k_{diss} with the respective proportion.

DISCUSSION

The results shown in Fig. 2 indicate that for substances injected into the vitreous of rabbit eyes their dissipation rates, and with this also the vitreal half-lives, are determined by one of the three possible transport mechanisms discussed above, depending mainly on the molecular weight of the substance. Very low MW ($< 350 \text{ Da}$) substances are obviously efficiently absorbed at the back of the eye and therefore the radial diffusion to the border of the vitreous body is the rate limiting step for these drugs. This was concluded from the fact that for the

respective substances the dissipation rates could be well predicted with an equation describing this process based on a reasonable assumption for the thickness of depletion layer through which the molecules need to diffuse. Due to its steep MW dependence, the rate of permeation through BoE tissue is smaller than the rate of diffusion to BoE above a MW of 350 Da and thus for these larger molecules the uptake into the BoE tissue becomes the rate limiting step. The strong MW dependence of the dissipation rates following a power law with exponent around -6 gives rise to the conclusion that even the hydrophilic compounds in the present dataset permeate transcellularly through the BoE tissue. For paracellular permeation the MW dependence, as derived from the Renkin equation (27), is expected to be much shallower if typical radii of tight junctions in epithelial membranes are considered (for details see [suppl. material](#) provided online). For even larger molecules with a molecular weight of 500 Da and above, uptake into BoE becomes so slow that the alternative dissipation path, i.e. diffusion to the front of the eye and subsequent transport into the anterior chamber by the aqueous humor flow, is more efficient and thus becomes the predominant process. The flow rate of the aqueous ($Q = 3 \mu\text{L}/\text{min}$) is high enough that it could give rise to vitreal dissipation rates of $k_{\text{diss, aqueous}} = 0.13 \text{ 1/h}$ (with $V_d = 1.4 \text{ mL}$) which are larger than those observed for molecules with $\text{MW} > 500 \text{ Da}$. Therefore it must be concluded that the rate limiting step for transport to the front of the eye is the diffusion within the vitreous towards the posterior chamber. This is also supported by the observed molecular weight dependence of dissipation rates that hints to a diffusion process instead of a flow process, which would be independent of MW.

As can be seen from Fig. 2 this interpretation well explains the general MW dependence of the dissipation rates for the substances in the present dataset. Additionally, the fact that range in which the dissipation rates lie could be very well predicted from first principles by equations considering just passive diffusion allows for the conclusion that fluid flows, driven by convection of pressure gradients, do not contribute significantly to the dissipation of intravitreally applied drugs.

Despite the overall good agreement there remain several cases where the observed dissipation rates deviate strongly from the lines representing the calculated values. These discrepancies are partly caused by experimental uncertainties, given by the fact that the rates are not measured directly, but are calculated values derived by model based evaluations of time series data. Since the values are collected from many different studies, it also cannot be excluded that slightly different approaches for these evaluations result in significant variability. This interpretation is supported by the finding that for some substances more than one rate value was found, reported in different publications. The differences between these values typically make up a factor of two, but in at least one

case an almost fourfold difference between the smallest and the largest value was found.

Apart from this, there are deviations from the predicted equations which may be explained by processes influencing dissipation from the vitreous and are being ignored or not considered in the simplified equations used. For small molecules ($\text{MW} < 500 \text{ Da}$), this is mainly the ignorance of the influence of unbound fractions and partition coefficients. Setting the volume of distribution to the physical volume of the vitreous, which is equivalent to assuming that the unbound fraction is one, has no major impact for the present dataset. All substances in the present data set with respectively low MWs are actually low lipophilic or even hydrophilic, meaning that the assumption of a fraction unbound close to one is valid. However, for some of the substances with $\text{MW} < 350 \text{ Da}$, logD values one to several orders of magnitude lower compared to the other substances with a similar MW are reported (i.e. Forscarnet, Cidofovir, Fluorouridine-50 phosphate, marked by open circles in Fig. 2). For these cases, also extremely small partition coefficients between cell membranes and water ($K_{m:w}$) would be expected with the consequence of significantly reduced rates of permeation through BoE, then potentially facilitated by paracellular diffusion. This then leads to the fact that no longer the diffusion within the vitreous is the rate limiting process but rather the absorption or alternatively the dissipation via the anterior route. Consequently, rates of dissipation for these substances are observed which are 1 to 2 orders of magnitude lower than those calculated with Eq. 11. Also for substances in the medium MW range a dependence of permeability on lipophilicity can be expected and was experimentally confirmed with a single study with chemically similar substances (28). Here, however, the methodological uncertainty in the dissipation rate values and the fact the only logP values and not the partition coefficients at the vitreal pH were consistently available, hampered the inference of this dependence within the observed variability.

In contrast, for four substances in the high molecular weight range, much higher than expected dissipation rates are reported. These are three FITC-dextranes of different molecular weights and VEGF (marked by open squares in Fig. 2). For all four of these substances, the observed rates are very close to those which would result if the substances would be absorbed into the BoE efficiently and the transport there was limiting the dissipation. It is not quite clear how this finding could be explained and it can only be speculated that uptake of these substances into the retina is facilitated by other, more effective routes than passive paracellular transport. It can also not be excluded that the respective compounds are chemically instable in the vitreous and their metabolic rates just coincide with the rates of diffusion to back of the eye.

The equations presented here can easily be used for predicting vitreal half-lives, in particular in early development of intraocular drugs without a need for complex mathematical

models or expensive software. Due to the simplicity of the calculations, the predictions can even be derived using a spread sheet and could be determined for a large number of compounds simultaneously. In addition, the analyses contribute to a mechanistic understanding of which transport process is relevant for the dissipation from the vitreous depending on the substance properties. This provides an advantage in early development by refining *in vitro* experiments, optimizing study design and accelerating the pre-clinical development phase which would therefore save time and money.

While the method described here was optimized to estimate vitreal half-lives in the rabbit eye, the equations could be easily translated to humans. It can be assumed that the basic principles and assumptions from the equations are the same for humans and rabbits with some small adjustments. The model equations contain geometrical factors of the eye and would therefore need to be adapted to the shape and geometry of the human eye. This could lead to different absolute values and moreover to different cutoff values for the molecular weights at which the transitions between the rate limiting transport processes occur, however the inclusion of the new values would not be complicated. Because many of the vision impairing disorders that affect the posterior region of the eye result in changes to the blood-ocular barriers, some factors may also need to be adjusted specifically for patient eyes. Patients with these diseases are often older and age-related liquefaction of the vitreous humor leads to reduced viscosity (29). In some diseases, such as wet AMD, the integrity of the BoE tissue layers is impaired and this may result in accelerated dissipation. Overall this is not expected to have a large impact on the prediction of vitreal half-lives, however is an aspect that should be considered.

CONCLUSION

A method to predict vitreal half-lives in the rabbit eye was developed based on simple equations describing the physical processes of dissipation by considering the physicochemical properties of ocular therapeutic substances. Substances injected into the vitreous of the eye are cleared from it either through the front of the eye by transport in the aqueous humor flow or through back of the eye by uptake into the tissue and evacuation with the blood flow, depending on the molecular weight of the substance. The respective dissipation rates are determined by different transport processes: very low MW substances are limited by diffusional transport to the back of the eye, substances with a MW >350 Da are limited by the uptake into the back of the eye tissue, and for even larger molecules >500 Da again the diffusion in the vitreous towards the front of the eye determines the dissipation rate. Using this model it is possible to reliably predict vitreal half-lives of a wide

range of substances and could simplify and improve the early clinical development of intraocular compounds.

The present study has several limitations. The fact that the experimental data were collected from different literature sources leads to some uncertainty concerning the comparability of the values. Although the dataset is considerably large with a high diversity in the properties of the compounds, there are only substances in the low lipophilicity range included. Therefore the validity of the introduced equations for higher lipophilic substances could not be tested. Finally the model is only valid for rabbit eyes. Although a path forward to translation to the human setting was given, it could not be tested if an adapted model has the same predictivity for human vitreal half-lives, due to the lack of sufficient experimental data.

ACKNOWLEDGMENTS AND DISCLOSURES

The author thanks Anne von Bodman for her writing support. Likewise the critical questions and suggestion of the reviewers are acknowledged, which helped to improve the manuscript very much in a revised version.

REFERENCES

- Zhang K, Zhang L, Weinreb RN. Ophthalmic drug discovery: novel targets and mechanisms for retinal diseases and glaucoma. *Nat Rev Drug Discov.* 2012;11:541–59.
- del Amo EM, Urtti A. Current and future ophthalmic drug delivery systems. A shift to the posterior segment. *Drug Discov Today.* 2008;13:135–43.
- Washington N, Washington C, Wilson C. *Physiological pharmaceutics: barriers to drug absorption.* 2nd ed. London: Taylor and Francis; 2001.
- Del Amo EM, Vellonen KS, Kidron H, Urtti A. Intravitreal clearance and volume of distribution of compounds in rabbits: In silico prediction and pharmacokinetic simulations for drug development. *Eur J Pharm Biopharm.* 2015;95:215–26.
- Durairaj C, Shah JC, Senapati S, Kompella UB. Prediction of vitreal half-life based on drug physicochemical properties: Quantitative Structure–Pharmacokinetic Relationships (QSPKR). *Pharm Res.* 2009;26:1236–60.
- Haghjau N, Abdekhodaie MJ, Cheng YL. Retina-choroid-sclera permeability for ophthalmic drug in the vitreous to blood direction: quantitative assessment. *Pharm Res.* 2013;30:41–59.
- Haghjau N, Abdekhodaie MJ, Cheng YL, Saadatmand M. Computer modeling of drug distribution after intravitreal administration. *World Acad Sci Eng Technol.* 2011;5:601–11.
- Missel PJ. Hydraulic flow and vascular clearance influences on intravitreal drug delivery. *Pharm Res.* 2002;19:1636–47.
- Stay MS, Xu J, Randolph TW, Barocas VH. Computer simulation of convective and diffusive transport of controlled-release drugs in the vitreous humor. *Pharm Res.* 2003;20:96–102.
- Missel PJ. Simulating intravitreal injections in anatomically accurate models for rabbit, Monkey, and human eyes. *Pharm Res.* 2012;29:3251–72.
- Ahn J, Hyuncheol KH, Woo SJ, Park JH, Park S, Hwang DJ, *et al.* Pharmacokinetics of intravitreally injected bevacizumab in vitrectomized eyes. *J Ocul Pharmacol Ther.* 2013;29:612–8.

12. Maurice DM, Mishima S. Ocular pharmacokinetics. In: Sears L, editor. *Pharmacology of the eye*. Berlin: Springer; 1984.
13. Moseley H, Foulds HW, Allan D, Kyle PM. Routes of clearance of radioactive water from the rabbit vitreous. *Br J Ophthalmol*. 1984;68:145–51.
14. Laurent UBG, Fraser JRE. Turnover of hyaluronate in the aqueous humor and vitreous body of the rabbit. *Exp Eye Res*. 1983;36:493–504.
15. Wishart DS, Knox C, Guo AC, Shrivastava S, Hassanali M, Stothard P, *et al*. DrugBank: a comprehensive resource for in silico drug discovery and exploration. *Nucleic Acids Res*. 2006;34(Database issue):D668–72. 16381955.
16. Lieb WR, Stein WD. The molecular basis of simple diffusion within biological membranes. In: Bronner F, Kleinzeller A, editors. *Current topics in membranes and transport*, vol. 2. New York: Academic; 1971.
17. Polson A. Some aspects of diffusion in solution and a definition of a colloidal particle. *J Phys Chem*. 1950;54:649–52.
18. Abdelkawi SA, Abdel-Salam AM, Ghoniem DF, Ghaly SK. Vitreous humour rheology after Nd:YAG laser photo disruption. *Cell Biochem Biophys*. 2014;68:267–74.
19. Reichenbach A, Schnitzer J, Friedrich A, Ziegert W, Brückner G, Schober W. Development of rabbit retina, I. Size of eye and retina, and postnatal cell proliferation. *Anat Embryol*. 1991;183:287–97.
20. Collander R, Bärlund H. Permeabilitätsstudien an Chara Ceratophyllia. *Acta Bot Fenn*. 1933;11:1–114.
21. Levin VA, Dolginov D, Landahl L, Yorke C, Csetjey J. Relationship of octanol/water partition coefficient and molecular weight to cellular permeability and partitioning in S49 lymphoma cells. *Pharm Res*. 1984;1:259–66.
22. Lieb WR, Stein WD. Biological membranes behave as non-porous polymeric sheets with respect to the diffusion of non-electrolytes. *Nature*. 1969;224:240–3.
23. Schmitt W. General approach for the calculation of tissue to plasma partition coefficients. *Toxicol in Vitro*. 2008;22:457–67.
24. Kleinberg TT, Tzekov RT, Stein L, Ravi N, Kaushal S. Vitreous substitutes: a comprehensive review. *Surv Ophthalmol*. 2011;56:300–23.
25. Kim JO, Cotlier E. Phospholipid distributions and fatty acid composition of lysophosphatidylcholine and phosphatidylcholine in rabbit aqueous humor, lens and vitreous. *Exp Eye Res*. 1976;22:569–76.
26. Keldenich J, Schmitt W, Willmann S. A physiological model for predicting organ/plasma partitioning and volume of distribution. In: Testa B, Krämer SD, Wunderli-Allensbach H, Folkers G, editors. *Biological and physicochemical profiling in drug research*. VHC A, Zurich, and Wiley-VCH, Weinheim; 2004.
27. Renkin EM. Filtration, diffusion, and molecular sieving through porous cellulose membranes. *J Gen Physiol*. 1954;38:225–43.
28. Liu W, Liu QF, Perkins R, Drusano G, Louie A, Madu A, *et al*. Pharmacokinetics of sparfloxacin in the serum and vitreous humor of rabbits: physicochemical properties that regulate penetration of quinolone antimicrobials. *Antimicrob Agents Chemother*. 1988;42:1417–23.
29. Laude A, Tan LE, Wilson CG, Lascaratos G, Elashry M, Aslam T, *et al*. Intravitreal therapy for neovascular age-related macular degeneration and inter-individual variations in vitreous pharmacokinetics. *Prog Retin Eye Res*. 2010;29:466–75.